

RSC Advances



This is an *Accepted Manuscript*, which has been through the Royal Society of Chemistry peer review process and has been accepted for publication.

Accepted Manuscripts are published online shortly after acceptance, before technical editing, formatting and proof reading. Using this free service, authors can make their results available to the community, in citable form, before we publish the edited article. This *Accepted Manuscript* will be replaced by the edited, formatted and paginated article as soon as this is available.

You can find more information about *Accepted Manuscripts* in the [Information for Authors](#).

Please note that technical editing may introduce minor changes to the text and/or graphics, which may alter content. The journal's standard [Terms & Conditions](#) and the [Ethical guidelines](#) still apply. In no event shall the Royal Society of Chemistry be held responsible for any errors or omissions in this *Accepted Manuscript* or any consequences arising from the use of any information it contains.

Thermoresistive properties of p-type 3C-SiC nanoscale thin films for high-temperature MEMS thermal-based sensors†

Toan Dinh,^{*a,†} Hoang-Phuong Phan,^{a,†} Takahiro Kozeki,^b Afzaal Qamar,^a Takahiro Namazu,^b Nam-Trung Nguyen,^a and Dzung Viet Dao^{a,c}

Received * * 2015

DOI: 10.1039/b000000x

We report for the first time the thermoresistive property of p-type single crystalline 3C-SiC (p-3C-SiC), which was epitaxially grown on a silicon (Si) wafer, and then transferred to a glass substrate using a Focused Ion Beam (FIB) technique. A negative and relatively large temperature coefficient of resistance (TCR) up to -5500 ppm/K was observed. This TCR is attributed to two activation energy thresholds of 45 meV and 52 meV, corresponding to temperatures below and above 450 K, respectively, and a small reduction of hole mobility with increasing temperature. The large TCR indicates the suitability of p-3C-SiC for thermal-based sensors working in high-temperature environments.

In recent years, silicon carbide (SiC) has emerged as an appropriate material for high-temperature electronics thanks to its superior properties, such as large band gap and high thermal conductivity¹⁻⁴. To date, more than 200 SiC polytypes such as 3C, 4H and 6H have been discovered^{5,6}. Among these polytypes, single crystalline 3C-SiC, with its capability of being grown on a large-diameter silicon (Si) wafer (e.g. 300 mm), is one of the main technological polytypes⁷⁻⁹. Thanks to its high temperature coefficient of resistance (TCR)¹⁰, large band gap¹¹ and fast thermal response¹², 3C-SiC would be a good material for developing thermal sensors such as temperature sensors^{13,14}, flow sensors¹⁵⁻¹⁷, inertial sensors^{18,19} and micro-heaters^{10,20}. In addition, the operation of thermal-based sensors (e.g. thermal flow sensors and convective accelerometers) relies on the Joule heating effect, which requires a low resistivity for small supply voltage and ease of detection. Consequently, crystalline SiC is a suitable choice for such applications. This material can also be employed for thermal-based sensors integrated with on-chip electronic devices. Further-

more, the low substrate conductivity is a crucial property for the operation of such SiC thermal sensors^{10,21}. However, both the vertical current leakage and the degrading electrical property of the silicon (Si) substrate at high temperatures limit the applications of 3C-SiC on Si platforms for high-temperature electronic devices^{22,23}. A solution for this problem is transferring SiC onto an insulating substrate. Characterizing the thermoresistive property of the transferred SiC film is of great interest for practical applications.

Since single crystalline 3C-SiC cannot be grown on any insulating substrates, recent research has focused on transferring techniques such as Smart Cut²⁴ and wafer bonding²⁵, to create high-quality single crystalline 3C-SiC thin films on insulating substrates. However, these techniques suffer several disadvantages such as implantation damage and a limitation of the implanted oxide layer thickness.

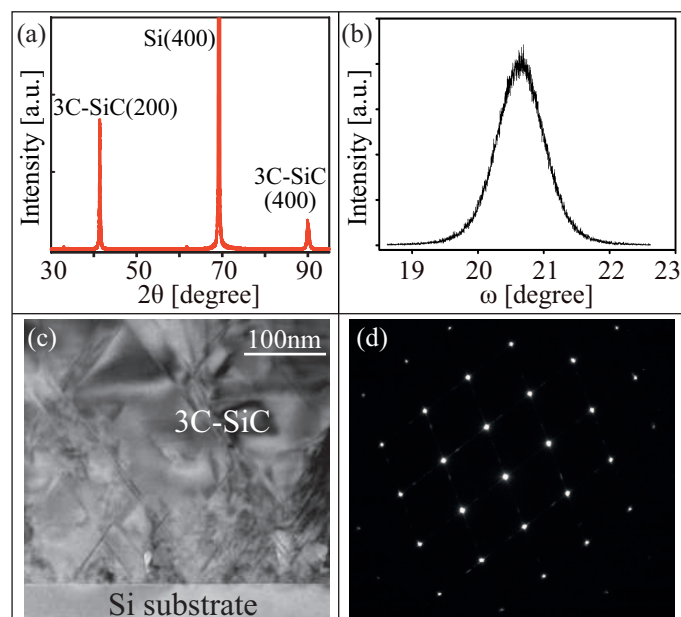


Fig. 1 Characteristics of the SiC film: (a) The XRD graph of p-3C-SiC grown on (100) Si; (b) The rocking curve scan of 3C-SiC; (c) The TEM image of 3C-SiC; (d) The SAED image of 3C-SiC. (Reproduced with permission from ref. 26. Copyright [2014], AIP Publishing LLC.)

* Email of corresponding author: toan.dinh@griffithuni.edu.au

^a Queensland Micro- and Nanotechnology Centre, Griffith University, Brisbane Queensland 4111, Australia.

^b Department of Mechanical Engineering, University of Hyogo, Hyogo, Japan.

^c School of Engineering, Griffith University, Queensland, Australia.

† Toan Dinh and Hoang-Phuong Phan contributed equally to this work.

† Electronic Supplementary Information (ESI) available: The fabrication processes, experimental setup for thermoresistive characterization, the current flow in p-3C-SiC on Si, and the impact of thermoelectric effect. See DOI: 10.1039/c000000x/

In this paper, we report the growth of the p-3C-SiC on Si wafer by Low-Pressure Chemical Vapour Deposition (LPCVD) and the subsequent transfer of the SiC thin film to a glass substrate using the Focused Ion Beam (FIB) technique. We characterized the thermoresistive properties of this material and observed a relatively high temperature coefficient of resistance (TCR). We also demonstrated the use of p-3C-SiC on SiO₂ as a suitable material system for high-temperature thermal-based sensors.

The LPCVD process was performed at a temperature of 1273 K to grow p-3C-SiC nanoscale thin films with a thickness of 280 nm on (100) Si substrate. Silane (SiH₄) and propylene (C₃H₆) were employed as alternating precursors. To form p-type SiC material, the trimethylaluminum [(CH₃)₃Al, TMAI] precursor was exploited in the *in situ* doping process. Figure 1(a) shows the full-range of X-Ray Diffraction (XRD) measurement, indicating the growth of 3C-SiC on Si. The full width at half maximum (FWHM) of approximately 0.8 de-

gree was observed (Fig. 1(b)). Furthermore, the Transmission Electron Microscope (TEM) image (Fig. 1(c)) indicates good crystallinity of the as-grown SiC film. In addition, the selected area electron diffraction (SAED) (Fig. 1(d)) confirms the single crystalline characteristics of the as-grown SiC film.

The Hall measurement was also performed to determine the carrier concentration of the films at room temperature (~300 K). The obtained results indicate a carrier concentration of $5 \times 10^{18} \text{ cm}^{-3}$ for the as-grown SiC films. In addition, the resistivity of the p-3C-SiC films was measured to be approximately $0.14 \text{ } \Omega \text{ cm}^{-1}$. This resistivity is in the common range used for thermal-based sensors¹⁰. We also investigated the current flow in p-3C-SiC on a Si substrate as a reference (ESI†). The results indicate that p-3C-SiC on a Si substrate is not a good choice for thermal-based sensors at temperatures higher than 350 K. Therefore, we transferred the p-3C-SiC onto SiO₂ and then examined its thermoresistive property for a temperature range of 300 to 600 K, which will be presented hereafter.

We formed the I-shaped SiC resistors on the Si substrate using standard photolithography and dry etching processes^{28,29} (ESI†), Fig. 2(a). Aluminum electrodes were used for making the Ohmic contacts between the SiC films and the subsequent deposited tungsten. We then released the SiC resistors from the substrate, employing an isotropic dry etching process with XeF₂ as the etching gas³⁰ (ESI†), Fig. 2(b). Next, we utilized FIB to remove the SiC films from the Si substrate, Fig. 2(c). A micro probe (ESI†) was then employed to transfer the SiC resistors onto a SiO₂ substrate where aluminum electrodes were readily deposited, Fig. 2(d). Finally, a tungsten layer was deposited to fix the SiC films on the SiO₂ substrate, Fig. 2(e). Figure 2(f) shows a scanning electron microscope (SEM) image of a SiC resistor after it was transferred to the insulating substrate.

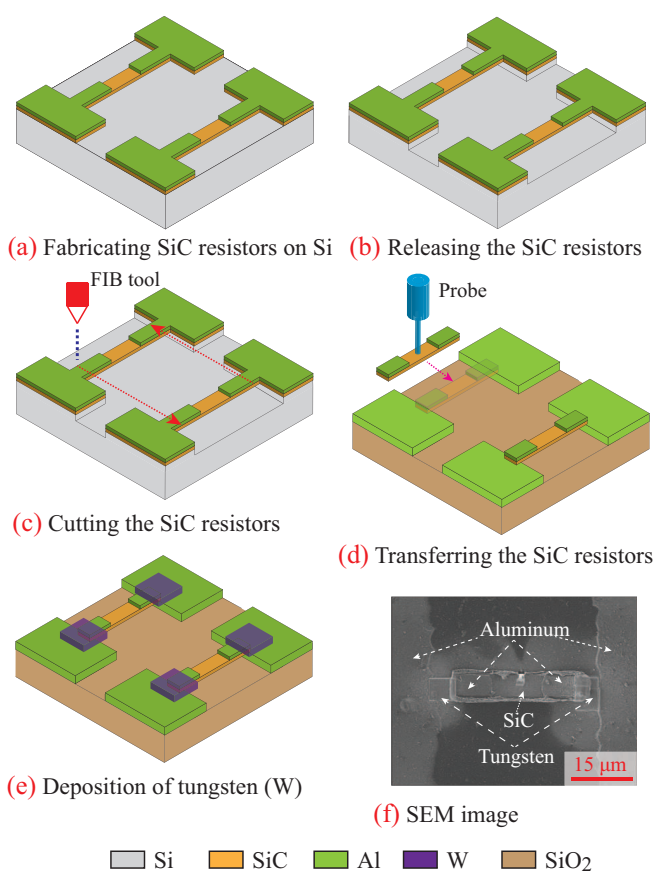


Fig. 2 Fabrication steps of p-3C-SiC on SiO₂: (a) Fabrication of p-3C-SiC on Si substrates; (b) Releasing the SiC structures; (c) Cutting the SiC resistors using a Focused Ion Beam (FIB) method; (d) Transferring the SiC onto a SiO₂ substrate; (e) Deposition of tungsten (W); (f) Scanning Electron Microscopy (SEM) image of p-3C-SiC on SiO₂.

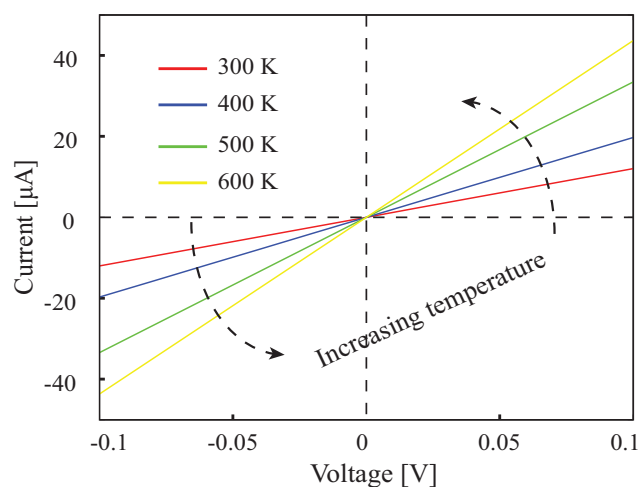


Fig. 3 The current-voltage (IV) characteristic of p-3C-SiC on SiO₂ substrate measured at different temperatures.

An experimental setup was established for the thermoresistive characterization of the p-3C-SiC films (ESI†)¹³. Figure 3 shows the typical current-voltage (I-V) curves of the p-3C-SiC film at various temperatures ranging from room temperature of 300 K to 600 K. The applied voltage varied from -0.1 V to 0.1 V. The I-V curves show that a good contact between the aluminum electrodes and the p-type 3C-SiC was maintained in the whole temperature range. The I-V data also indicate that the conduction of SiC is thermally activated, because impurities are ionized with increasing temperature. In addition, the thermoelectric effect of the Al-W junction can be neglected because the temperature distribution of the device is expected to be uniform. This assumption is experimentally supported by the fact that the linear I-V curves pass through the origin at elevated temperatures (Fig. 3, ESI†).

Fig. 4(a) shows the resistance values derived from the I-V data. The resistance decreases significantly with increasing temperature (*e.g.* up to 80% at 600 K). As a result, the measured temperature coefficient of resistance (TCR) varies from -2400 ppm/K to -5500 ppm/K, Fig. 4(b). This TCR is comparable to that of other thermal sensing materials such as platinum (3920 ppm/K).

The p-type 3C-SiC doped with a concentration of $5 \times 10^{18} \text{ cm}^{-3}$ possesses sensitive ionization characteristics with increasing temperature, evident through the significant increase of its conductivity. We hypothesise that the free hole concentration (n) increases with increasing temperature, and remains constant once the impurities are fully ionized. Therefore, the absolute TCR is large near room temperature and decreases with increasing temperature as a result of the decrease in the hole mobility. The temperature dependence of hole concentration in p-3C-SiC can be expressed as^{31,32}:

$$n \sim T^{3/2} \exp\left(-\frac{E_a}{kT}\right) \quad (1)$$

where E_a is the activation energy of the acceptor (hole), and k is the Boltzmann constant. In addition, the hole mobility decreases with increasing temperature and can be simply determined as³³⁻³⁵:

$$\mu \sim T^{-\alpha} \quad (2)$$

where α is an experimental constant. The resistivity (ρ) of the SiC films can be determined from the hole concentration (Eq. 1) and its mobility (Eq. 2) using Eq. 3 as follows:

$$\rho = \frac{1}{q\mu n} \sim T^{\alpha-3/2} \exp\left(\frac{E_a}{kT}\right) \quad (3)$$

where q is the electron charge. Deducing from Eq. (3), the relationship between the resistance change and the temperature can be written in the following form:

$$\ln\left(\frac{R}{R_0}\right) = \left(\alpha - \frac{3}{2}\right) \ln\left(\frac{T}{T_0}\right) + E_a \left(\frac{1}{kT} - \frac{1}{kT_0}\right) \quad (4)$$

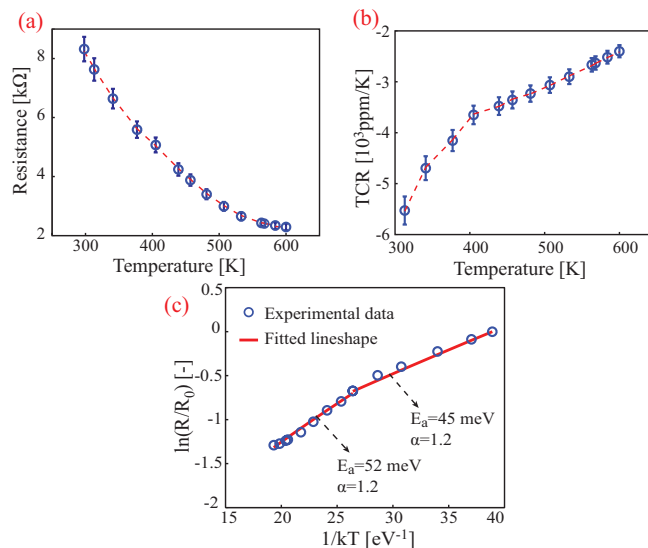


Fig. 4 Thermoresistive characteristics of the p-3C-SiC on SiO₂ platform: (a) Electrical resistance versus temperature (Number of samples N=4); (b) Temperature coefficient of resistance (TCR) of the p-3C-SiC material; (c) Non-linear Arrhenius plot of the p-3C-SiC thermoresistance and its fitting curves.

where R_0 is the SiC resistance at the reference temperature T_0 . Figure 4(c) shows the non-linear Arrhenius plot of the p-3C-SiC and its fitted curves based on Eq. 4. The hole mobility constant was found to be 1.2, and two activation energy thresholds of 45 meV and 52 meV were extracted, corresponding to temperature ranges of 300 K to approximately 450 K and 450 K to 600 K, respectively. These low activation energy thresholds were found, which are due to the fact that the doped SiC film has a large hole concentration ($5 \times 10^{18} \text{ cm}^{-3}$). At this concentration, the impurities are partly ionized at room temperature. Thus, the Fermi level becomes closer to the valence band of SiC. In addition, as the low activation energy thresholds of 45 meV and 52 meV were found, it is likely that the holes from the acceptor levels require a small increase in thermal energy to be activated into the top edge of the valence band. Since the energy band gap of the 3C-SiC material is approximately 2.3 eV,³⁶ the calculated ratio of $2E_a/E_g$ was much smaller than the unity, indicating that the Fermi level is deeply located in the lower region of the forbidden band. It is also important to note that the scattering mechanism cannot be neglected, since the phonon scattering $\mu \sim T^{-1.2}$ limits the decrease in the resistivity of the SiC film at high temperatures.

In conclusion, we investigated the thermoresistive properties of p-3C-SiC grown on Si substrate, peeled off by FIB, and subsequently transferred on to a glass substrate. We then studied the conduction mechanism of the SiC material and found two low activation energy thresholds of 45 meV and 52 meV, as well as a temperature dependent mobility of $\mu \sim T^{-1.2}$. A negative and large TCR up to -5500 ppm/K was also obtained, demonstrating the feasibility of using this material for

thermal-based sensors working in high-temperature environments.

This work was performed in part at the Queensland node of the Australian National Fabrication Facility, a company established under the National Collaborative Research Infrastructure Strategy to provide nano and micro-fabrication facilities for Australia's researchers. This work has been partially supported by the Griffith University's New Researcher Grants and Australian Research Council grant LP150100153.

References

- 1 M. Mehregany, C. Zorman, N. Rajan, C. H. Wu, *Proceedings of the IEEE*, 1998, **86**(8), 1594.
- 2 V. Cimalla, J. Pezoldt and O. Ambacher, *J. Phys. D: Appl. Phys.*, 2007, **40**, 6386.
- 3 H.P. Phan, D.V. Dao, K. Nakamura, S. Dimitrijević, and N.T. Nguyen, *JMEMS*, 2015, DOI 10.1109/JMEMS.2015.2470132.
- 4 H. P. Phan, D. V. Dao, L. Wang, T. Dinh, N. T. Nguyen, A. Qamar, P. Tanner, S. Dimitrijević and Y. Zhu, *J. Mater. Chem. C*, 2015, **3**(6), 1172.
- 5 A. Qamar, P. Tanner, D. V. Dao, H. P. Phan, T. Dinh, *Electron Device Letters*, 2014, **35**(12), 1293.
- 6 A. Qamar, D. V. Dao, P. Tanner, H. P. Phan, T. Dinh, and S. Dimitrijević, *Applied Physics Express*, 2015, **8**(6), 061302.
- 7 L. Wang, S. Dimitrijević, J. Han, P. Tanner, A. Iacopi, and L. Hold, *Journal of Crystal Growth*, 2011, **329**(1), 67.
- 8 H. P. Phan, D. V. Dao, P. Tanner, L. Wang, N. T. Nguyen, Y. Zhu, S. Dimitrijević, *Appl. Phys. Lett.*, 2014, **104**(11), 111905.
- 9 H. P. Phan, P. Tanner, D. V. Dao, L. Wang, N. T. Nguyen, Y. Zhu, S. Dimitrijević, *Electron Device Lett.*, 2014, **35**(3), 399.
- 10 S. Noh, J. Seo, and E. Lee, *Trans. Electr. Electron. Mater.*, 2009, **10**, 131.
- 11 X. Lin, S. Lin, Y. Xu, A. A. Hakro, T. Hasan, B. Zhang, and H. Chen, *J. Mater. Chem. C*, 2013, **1**(11), 2131.
- 12 C. Lyons, A. Friedberger, W. Welser, G. Muller, G. Krotz, and R. Kassing, *Proc. Micro Electro Mechanical Systems*, 1998, 356.
- 13 T. Dinh, D. V. Dao, H. P. Phan, L. Wang, A. Qamar, N. T. Nguyen, P. Tanner, and M. Rybachuk, *Appl. Phys. Express*, 2015, **8**, 061303.
- 14 C. Yan, J. Wang, and P. S. Lee, *ACS nano*, 2015, **9**(2), 2130-2137.
- 15 T. Dinh, H. P. Phan, D. V. Dao, P. Woodfield, A. Qamar and N. T. Nguyen, *J. Mater. Chem. C*, 2015, DOI 10.1039/C5TC01650A
- 16 N.T. Nguyen, *IEEE Sensors J.*, 2005, **5**, 1224-1234.
- 17 W. C. Lin, M. A. Burns, *Analytical Methods*, 2015, **7**(9), 3981.
- 18 V. T. Dau, D. V. Dao, and S. Sugiyama, *Smart Mater. and Struct.*, 2007, **16**, 2308-2314.
- 19 D. V. Dao, V. T. Dau, T. Shiozawa, and S. Sugiyama, *JMEMS*, 2007, **16**, 950-958.
- 20 V. T. Dau, D. V. Dao, T. Yamada, B. T. Tung, K. Hata and S. Sugiyama, *Smart Mater. and Struct.*, 2010, **19**(7), 075003.
- 21 J. T. W. Kuo, L. Yu, and E. Meng, *Micromachines*, 2012, **3**, 550-573.
- 22 C. Dezaudier, N. Becourt, G. Arnaud, S. Contreras, J. L. Ponthenier, J. Camassel and C. Jaussaud, *Sensor Actuat. A-Phys.*, 1995, **46**(1), 71.
- 23 F. Maily, A. Giani, R. Bonnot, P. Temple-Boyer, F. Fascal-Delannoy, A. Foucaran, and A. Boyer, *Sensor Actuat. A-Phys.*, 2001, **94**, 32-38.
- 24 L. Di Cioccio, F. Letertre, Y. Le Tiec, A. M. Papon, C. Jaussaud, and M. Bruel, *Materials Science and Engineering: B*, 1997, **46**(1), 349.
- 25 Q. Y. Tong, U. Gosele, C. Yuan, A. J. Steckl, M. Reiche, *Journal of The Electrochemical Society*, 1995, **142**(1), 232.
- 26 H. P. Phan, D. V. Dao, P. Tanner, L. Wang, N. T. Nguyen, Y. Zhu, and S. Dimitrijević, *Applied Physics Letters*, 2014, **104**(11), 111905.
- 27 H. Yugami, S. Nakashima, A. Mitsuishi, A. Uemoto, M. Shigeta, K. Furukawa, and S. Nakajima, *Journal of applied physics*, 1987, **61**(1), 354.
- 28 A. Qamar, H. P. Phan, D. V. Dao, P. Tanner, T. Dinh, L. Wang, and S. Dimitrijević, *Electron Device Letters*, 2015, **36**(7), 708.
- 29 H. P. Phan, A. Qamar, D. V. Dao, T. Dinh, L. Wang, J. Han and N. T. Nguyen, *RSC Advances*, 2015, **5**(69), 56377.
- 30 D. Xu, B. Xiong, G. Wu, Y. Wang, X. Sun and Y. Wang, *J. Microelectromechanical Systems*, 2012, **21**(6), 1436.
- 31 S. O. Kasap, Semiconductor, *Principles of Electronic Materials and Devices*, New York, NY: McGraw-Hill, 2006, 373.
- 32 S. S. Li and W. R. Thurber, *Solid-State Electronics*, 1977, **20**(7), 609.
- 33 S. O. Kasap, Electrical and thermal conduction in solids, *Principles of Electronic Materials and Devices*, New York, NY: McGraw-Hill, 2006, pp. 113.
- 34 M. Roschke and F. Schwier, *IEEE Transactions on Electron Devices*, 2001, **48**(7), 1442.
- 35 K. Sasaki, E. Sakuma, S. Misawa, S. Yoshida, and S. Gonda, *Applied physics letters*, 1984, **45**(1), 72.
- 36 R. G. Humphreys, D. Bimberg and W. J. Choyke, *Solid St. Commun.*, 1981, **39**, 163.